Geophysical Research Letters

RESEARCH LETTER
10.1029/2025GL117956

Key Points:

- Multi-scale scattering and absorption tomography for detecting fractured and fluid-rich crustal volumes
- The first sensitivity test of absorption tomography in detecting known underground fluids in a tectonic environment
- Complex fluid dynamics trigger natural seismicity and influence the deformative behavior of the thrusts

Supporting Information:

Supporting Information may be found in the online version of this article.

Correspondence to:

R. de Nardis,
rita.denardis@unich.it

Citation:

Talone, D., Romano, M. A., De Siena, L., Guidarelli, M., Santulin, M., Peruzza, L., et al. (2025). Underground Gas Storage as benchmark for seismic attenuation tomography in a tectonically complex region (north-eastern Italy). *Geophysical Research Letters*, *52*, e2025GL117956. https://doi.org/10.1029/2025GL117956

Received 9 JUL 2025
Accepted 19 OCT 2025

Author Contributions:

Conceptualization: D. Talone, M. A. Romano, L. De Siena, R. de Nardis
Data curation: D. Talone, M. A. Romano, M. Guidarelli, M. Santulin, L. Peruzza
Formal analysis: D. Talone, M. A. Romano, R. de Nardis
Funding acquisition: M. A. Romano, L. Peruzza, R. de Nardis
Investigation: D. Talone, L. De Siena, R. de Nardis
Methodology: D. Talone, L. De Siena
Project administration: R. de Nardis
Resources: R. de Nardis
Software: L. De Siena
Supervision: M. A. Romano, L. De Siena, R. de Nardis
Validation: D. Talone, M. A. Romano, L. De Siena, G. Lavecchia, R. de Nardis

Underground Gas Storage as Benchmark for Seismic Attenuation Tomography in a Tectonically Complex Region (North-Eastern Italy)

D. Talone[1,2], M. A. Romano[3], L. De Siena[2,4], M. Guidarelli[3], M. Santulin[3], L. Peruzza[3], G. Lavecchia[1,2], and R. de Nardis[1,2]

[1]Department of Sciences, University of Chieti-Pescara "G. d'Annunzio", Chieti, Italy, [2]CRUST-Interuniversity Center for 3D Seismotectonics with Territorial Applications, Chieti, Italy, [3]National Institute of Oceanography and Applied Geophysics - OGS, Trieste, Italy, [4]Dipartimento di Fisica e Astronomia (DIFA), Alma Mater Studiorum-Università di Bologna, Bologna, Italy

Abstract We present a multiscale seismic attenuation tomography of a seismotectonically complex region in northern Italy hosting the well-characterized Collalto Underground Gas Storage (UGS). Beyond its specific relevance, this site provides a natural laboratory for assessing the ability of attenuation imaging to distinguish fluid-rich zones from highly strained, failure-prone volumes. We integrated scattering and absorption tomography models: scattering anomalies, between the two principal thrusts, highlight localized strain near fault tips; absorption tomography images the shallow UGS and reveals a deeper fluid-saturated volume. Seismicity concentrated around this deeper anomaly, exhibiting a pulsatory temporal pattern, suggests a fluid-driven role in the deformation processes. These findings show that attenuation tomography, combined with multiscale and complementary geophysical models, can resolve critical subsurface features related to fluids and strain. The approach is broadly applicable to geothermal and volcanic contexts and supports seismic hazard assessment in tectonically active regions where natural and anthropogenic processes may interact.

Plain Language Summary During their propagation, seismic waves change their amplitude and frequency content. By studying these variations, we can produce images of the energy lost by the waves due to the rock properties. Seismic attenuation and its two primary mechanisms, scattering and absorption, are sensitive to fluids, geochemistry, and temperature; however, they can also vary significantly due to rock heterogeneities and strain conditions. We tested the potential of these techniques in the Montello area (eastern Southern Alps, northern Italy), site of the Collalto Underground Gas Storage (UGS). The results confirm the position and geometry of the principal tectonic structures in the area and show the rock volume permeated by fluids (Collalto UGS). The absorption model also highlights a deeper, separated fluid reservoir, influencing the earthquakes release.

1. Introduction

The interplay between crustal fluids and tectonic stress is a critical factor in seismic hazard assessment, yet distinguishing their individual signatures in the subsurface remains a major challenge. Seismic attenuation, along with its two primary mechanisms (i.e., scattering and absorption) has proven highly effective for imaging subsurface heterogeneities in complex geological contexts (Borleanu et al., 2017; De Siena et al., 2017; Schurr et al., 2003). These methods are particularly sensitive to fluids, temperature, and strain, consistently with both laboratory (King, De Siena, Benson, & Vinciguerra, 2023) and numerical modeling simulations (Di Martino et al., 2022; King, De Siena, Zhang, et al., 2023).

Several studies associated attenuation anomalies with major fault systems, stress accumulation, and seismic activity or gaps (Gabrielli et al., 2023; Napolitano et al., 2020; Nardoni & Persaud, 2024; Talone et al., 2023). Nevertheless, attenuation imaging is still predominantly applied in volcanic environments (Clarke et al., 2020; Guardo et al., 2022; Prudencio et al., 2015; Reiss et al., 2022), where widespread fracturing, fluid circulation, and high strain rates favor strong attenuation contrasts. In such contexts, the sensitivity of seismic absorption to fluids is widely documented, for instance correlating high absorption values with melting portions of the lithosphere and reservoirs associated with volcanic activity (De Siena et al., 2016; Sketsiou et al., 2020). However, in tectonic settings, the straight correlation between attenuation and the presence of fluids remains debated. This is largely

Visualization: D. Talone
Writing – original draft: D. Talone
Writing – review & editing: D. Talone, M. A. Romano, L. De Siena, M. Guidarelli, G. Lavecchia, R. de Nardis

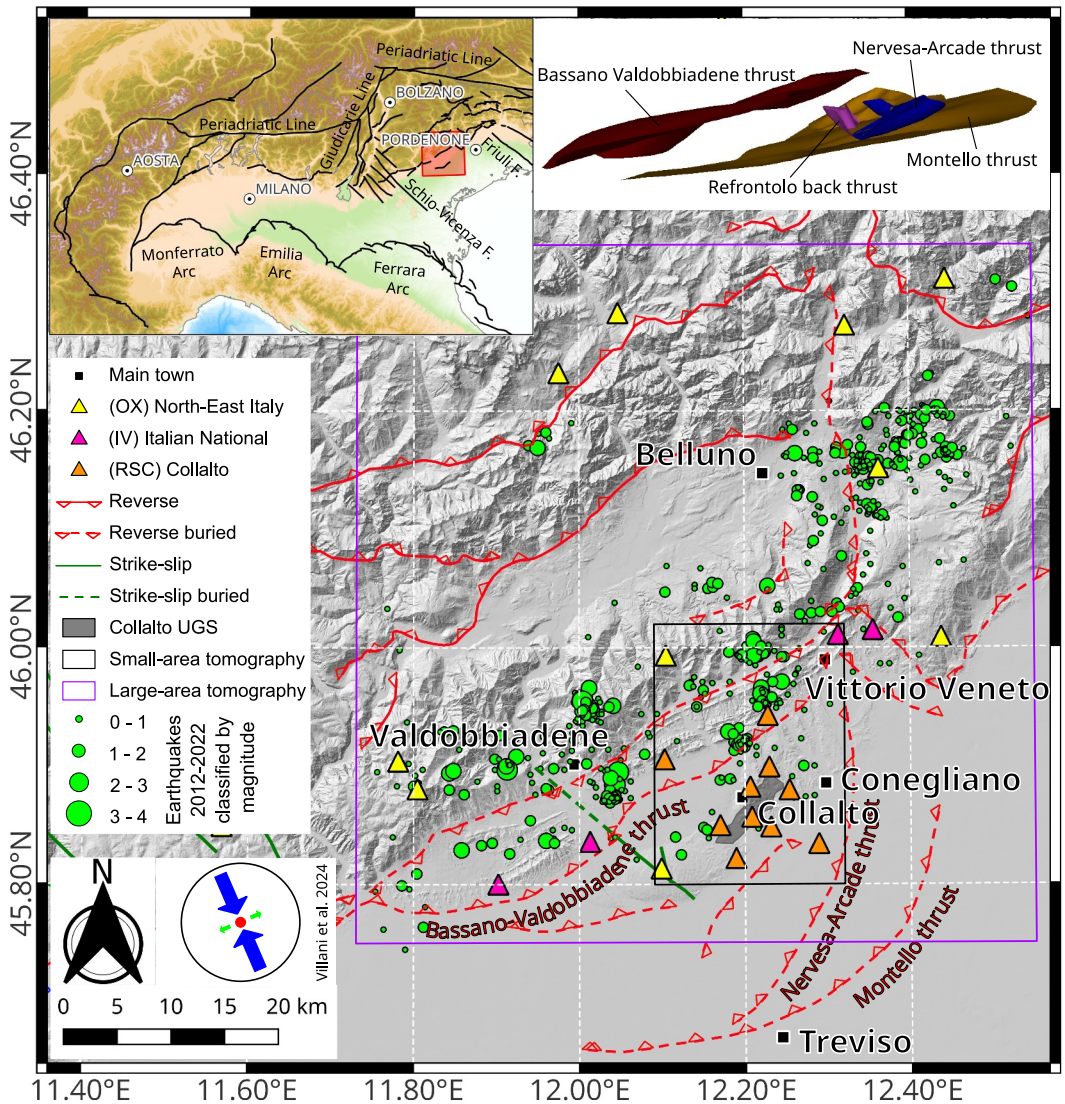

Figure 1. The seismotectonic framework of the Montello-Collalto area in the eastern Southern Alps (top-left inset shows the location map of the study area). Principal tectonic structures (Bigi et al., 1990; ITHACA Working Group, 2019; Picotti et al., 2022; SGI & UNMIG, 2010) are shown on the map and in a 3D view as reconstructed in this work (top-right inset). The available seismic stations (triangles) and seismic events (circles) from 2012 to 2022 are represented. The seismicity (sized according to the magnitude) corresponds to the catalog utilized for the tomography. Purple and black rectangles indicate the large and small tomography areas, respectively. Bottom-left inset displays the prevailing stress regime according to Villani et al. (2024).

due to trade-offs between absorption caused by the presence of fluids, distributed fracturing, and rock damage (e.g., Mavko et al., 2020; Zhu et al., 2021). As a result, attenuation anomalies are often difficult to interpret unambiguously in these contexts, especially when fluid pressure, strain localization, and lithologic contrasts coexist.

To address this issue, we perform an in situ benchmark test of multiscale attenuation tomography. We focus on the Montello thrust system, an active segment of the outer front of the eastern Southern Alps (SA) in Italy (Figure 1), which hosts the methane Collalto Underground Gas Storage (UGS) (Cargioli & Sola, 2007; Priolo et al., 2015). This site is particularly suitable for two reasons. First, the well-characterized UGS is an ideal reference target for evaluating the ability of attenuation imaging to discriminate between fluid- and strain-related anomalies at different scales. Second, the reservoir is embedded in a seismically active fold-and-thrust belt characterized by blind thrusts and interacting deformation processes.

Our results correlate well with the structural architecture proposed by Picotti et al. (2022), confirm the high-absorption signature of the UGS, and reveal a previously undetected deeper fluid-saturated volume. Its spatial correlation with local seismicity suggests that fluid circulation may modulate seismic behavior in the area, potentially supporting the hypothesis of a creep-like deformation regime as proposed in previous studies (Barba et al., 2013; Romano et al., 2019).

These findings have implications beyond the Montello-Collalto area, as they allow calibrating attenuation attributes with significant impact on seismic hazard assessment and resource management where imaging of fluids is central, like across geothermal reservoirs (Napolitano et al., 2025; Yemane et al., 2025). The ability to detect deep seismogenic sources supports studies in complex seismotectonic settings (Akinci et al., 2020, 2022; Visini et al., 2009, 2010) and seismic risk of carbon capture and storage sites (Tisato et al., 2015). Finally, they enhance our understanding of the role of deep fluids in earthquake cycles, including seismic swarms and aseismic creep along major faults (Reiss et al., 2022).

2. Seismotectonic Framework

The SA in northern Italy form an S-verging fold-and-thrust belt, a segment of the post-collision back thrusting zone of the Europe-verging Austroalpine-Penninic orogen (Castellarin et al., 2006). The eastern sector of the SA (Figure 1) is bounded by the Periadriatic Line (north) and by the Giudicarie Line (Castellarin et al., 2006; Curzi et al., 2024; Handy et al., 2010). The principal tectonic force driving the deformation of the belt is NNW-SSE compression (Villani et al., 2024) related to the collision of the Adria and European plates (Poli et al., 2008) (Figure 1). In this context, we focus on the Montello-Collalto area because of the coexistence of active tectonic structures, a high-quality local seismic network, and a well-known methane reservoir (Figure 1 and Figure S1 in Supporting Information S1).

The Montello thrust represents the outer front of the eastern SA (Picotti et al., 2022) and is characterized by an average shortening rate of about 0.3–0.4 mm/yr that is smaller than the Bassano-Valdobbiadene thrust behind it (Picotti et al., 2022). The two structures exhibit opposite deformation behaviors, characterized by a locked Bassano-Valdobbiadene thrust and a freely slipping Montello thrust (Barba et al., 2013; Picotti et al., 2022; Romano et al., 2019), as indicated by the velocity field (Anderlini et al., 2020).

The Montello hill hosts a methane reservoir, exploited between 1983 and 1994 (Cargioli & Sola, 2007), and converted into the Collalto UGS by Edison Stoccaggio S.p.A. (recently acquired by Snam). Since 2012, the National Institute of Oceanography and Applied Geophysics (OGS) has been in charge of the seismic monitoring of the Collalto UGS and the surrounding area, thanks to a local and permanent seismic network consisting of 10 stations with borehole sensors (Rete Sismica di Collalto [RSC], Figure 1) (Priolo et al., 2015). This high-resolution network plays a fundamental role in detecting several micro-earthquakes that are invisible to the regional and national seismic networks (Peruzza et al., 2022; Romano et al., 2019), thus filling a previously considered seismic gap (Burrato et al., 2008; Galadini et al., 2005).

A recent comprehensive analysis of the seismicity distribution in the Montello area is presented by Romano et al. (2019) for the period 1977–2017. The authors show predominantly sparse, low-energy (magnitude $\leq$4.0) seismicity between 5 and 15 km depth, which is classified as tectonically originated (Peruzza et al., 2022; Priolo et al., 2015; Romano et al., 2019). The dominant kinematics reflect a compressive response to the current deformation state (Villani et al., 2024), as confirmed by the available focal mechanisms (Saraò et al., 2021). An oblique-to-strike-slip component develops in response to deformation accommodation along high-angle secondary transverse structures, oriented NE-SW and NW-SE (Picotti et al., 2022; Romano et al., 2019). A stress inversion analysis performed by Romano et al. (2019) reveals general transcurrent kinematics in the westernmost area of the UGS, and reverse movement for the thrust-dominated Montello frontal zone. Peruzza et al. (2022) propose a mixed kinematics for the recent 2021 Refrontolo microseismic sequence, raising the question of local stress variations inducing oblique kinematics that accommodate the compressive push along pre-existing discontinuities.

3. Materials and Methods

The seismic catalog used in this study (January 2012–October 2022) comes from the RSC network. It comprises 1,326 micro-to-minor earthquakes with $0.0 \leq M_L \leq 3.9$, located with a 1D velocity model optimized for the

Montello-Collalto area (Romano et al., 2019) and characterized by the best hypocentral parameters according to Husen and Hardebeck (2010) criteria. We outlined two study areas: a small area centered on the Collalto UGS, and a large one encompassing the entire Montello thrust system. The completeness magnitude of the RSC catalog varies spatially (Mc 0.0 near the UGS and Mc 0.5 in the neighbors); thus, we removed all events with $M_L < 0.5$ to use a homogeneous catalog (Figure 1 and Figure S2 in Supporting Information S1). Finally, we obtained 689 earthquakes with 17,205 waveforms for the large area and 185 earthquakes with 6,777 records for the small area (Figure S3 in Supporting Information S1).

We performed a preliminary analysis following Talone et al. (2023). We considered four central frequency ranges to investigate the frequency content of seismic signals (1.5, 3, 6, and 12 Hz). Based on this analysis, we selected a central frequency of 12 Hz, which is appropriate given the small magnitudes of the earthquakes and the dimensions of the study area (Figures S4–S6 in Supporting Information S1). We then perform seismic scattering and absorption tomography with the Matlab© code MuRAT3D (De Siena et al., 2014). This code models the scattering (using the peak delay *PD* as a proxy) and absorption (using the inverse coda quality factor Qc^{-1} as a proxy) considering various portions of the seismogram (Reiss et al., 2022):

- Scattering is measured from the broadening envelope; *PD* corresponds to the time between T_0 (earthquake origin) and the maximum peak of the envelope (Aki & Chouet, 1975; Saito, 2002; Sato, 1989). Assuming that the wavelength is smaller than the correlation distance and that the propagation is constrained within a constant-velocity parallelepiped (average of the velocities encountered by the seismic ray), the method corrects for the increase in *PD* due to travel time and relates the remaining variations as scattering phenomena. The variations are allocated in the crossed blocks using the regionalization method, with the hit count serving as weights (Calvet et al., 2013; De Siena et al., 2016; Takahashi et al., 2009).
- Absorption is measured using the envelope decay of the coda waveform, starting from the results of a Multiple Lapse Time Window Analysis (Fehler et al., 1992). The sensitivity of the coda waves to the 3D Earth structure is evaluated using sensitivity kernels (Del Pezzo et al., 2018). MuRAT3D builds an inversion problem assuming that the measured coda energy is contained within the propagation grid (Sketsiou et al., 2020). Qc^{-1} becomes a proxy for absorption if coda waves are in the diffusive regime within a single high-diffusive layer. The code tests the equipartition between *P*- and *S*-wave energy by verifying the independence of coda attenuation from the hypocentral distance (Akande et al., 2019; De Siena et al., 2017; Mayor et al., 2016). This condition is sufficient to interpret Qc^{-1} absorption-related in the absence of leakage and coherent phases within the coda (Akande et al., 2019; Borleanu et al., 2023; Calvet et al., 2013; Napolitano et al., 2020; Nardoni et al., 2021; Sketsiou et al., 2020). Method's applicability and ray coverage have been properly tested (Figures S7–S9 in Supporting Information S1).

4. Results and Discussions

Recent studies (Picotti et al., 2022; Romano et al., 2019) have provided a comprehensive review of the geological and seismotectonic framework of the Montello thrust system. We combine 3D geological modeling with seismic scattering and absorption tomography to explore the relationship between attenuation anomalies and fault architecture, stress distribution, and fluid content. Major faults have been reconstructed by integrating geological, geophysical, and seismological data using the MOVE suite software (PetEx Ltd., version, 2022, 3D model in Figure 1). Our analysis starts with a look at regional-scale scattering anomalies and their tectonic implications. Then, we discuss localized variations in scattering and absorption, comparing them with existing models and seismicity patterns.

4.1. Scattering: Fracturing and Stress

Our results suggest that seismic scattering anomalies are closely related to major faults and the zones of strain accumulation. The regions of high scattering are located in the area between the hanging wall of the Montello thrust and the footwall of the Bassano–Valdobbiadene thrust (Figures S10–S12 in Supporting Information S1). This correlation highlights damage zones surrounding fault cores, as shown in cross-section A–A′ (Figure 2), where anomaly 1 broadens along the mapped thrust traces. Similarly, anomaly 2 aligns with the branching of the Nervesa–Arcade system from the Montello thrust, consistent with the expected increase in fracturing at fault junctions. These patterns agree with previous studies (Gabrielli et al., 2023; Napolitano et al., 2020) that associate high seismic scattering to high rock fracturing caused by tectonic deformation. Comparison with the geological

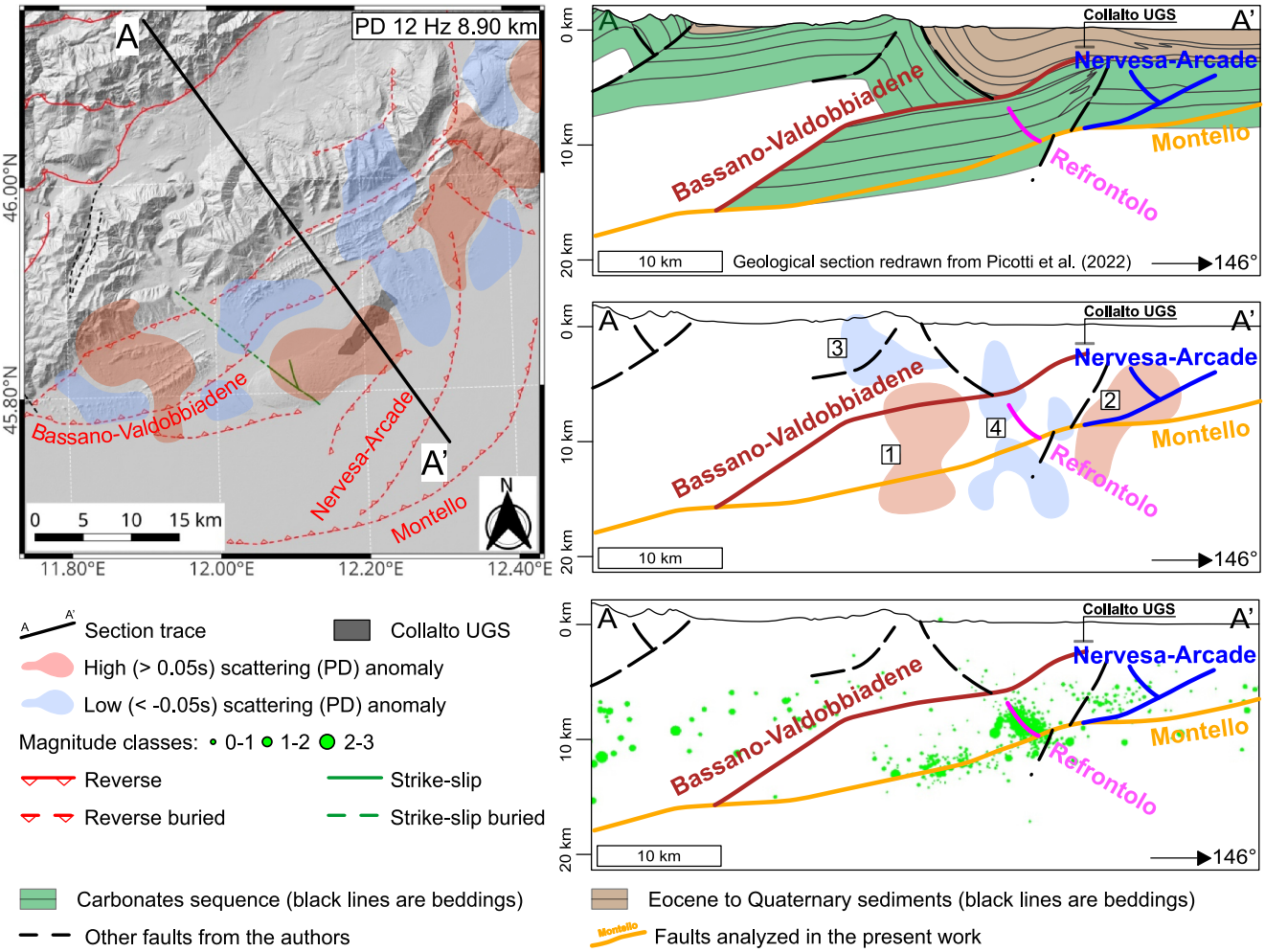

Figure 2. Scattering map and section from the *PD* tomography compared to geological, tectonic, and seismic features. The large-scale scattering model is represented as iso-surfaces, indicating peak delay values higher than +0.05 s (red) or lower than −0.05 s (blue), calculated at a central frequency of 12 Hz and depicted as a horizontal slice at a depth of 8.90 km. Anomalies are reported in the most constrained volume according to the seismic ray distribution (Figure S6 in Supporting Information S1). The vertical cross-section AA′ (represented in the map) is compared with the geological section CC′ in Picotti et al. (2022), which in turn has the same trace. The carbonate sequence and Eocene to Quaternary sediments are highlighted to underscore the main lithological variations. Fault traces from the same authors are represented: colors and labels have been attributed to the principal thrust discussed in this work. The position of the Collalto Underground Gas Storage (labeled black rectangle) is also shown. In the latter section seismicity represented in Figure 1 is projected with a semi-width of 5 km and scaled according to the magnitude.

model of Picotti et al. (2022) reveals that high-*PD* values are mainly concentrated in the carbonate units, likely reflecting their higher stiffness compared to the overlying sedimentary cover. This mechanical contrast enhances strain localization along fault planes and promotes seismic scattering (Atterholt et al., 2022; King, De Siena, Benson, & Vinciguerra, 2023).

In contrast, anomalies 3 and 4, although located within carbonates, show low scattering. These low-*PD* zones are associated in literature with areas of increased tectonic stress (Gabrielli et al., 2023; King, De Siena, Benson, & Vinciguerra, 2023; King, De Siena, Zhang, et al., 2023; Talone et al., 2023). Anomaly 3 occurs in the axial zone of a SE-verging overturned fold, where compressive stress likely deforms the heterogeneity, while fold limbs may remain more fractured. Anomaly 4 marks a stress accumulation zone along secondary structures of the Montello thrust, including the Refrontolo backthrust, and coincides with the 2021 Refrontolo seismic sequence. Minor discrepancies between scattering anomalies and mapped faults are likely due to tomographic resolution limitations and interpolation artifacts. Nevertheless, *PD* proves to be a robust proxy for delineating fault geometry and regional stress regimes.

10.1029/2025GL117956

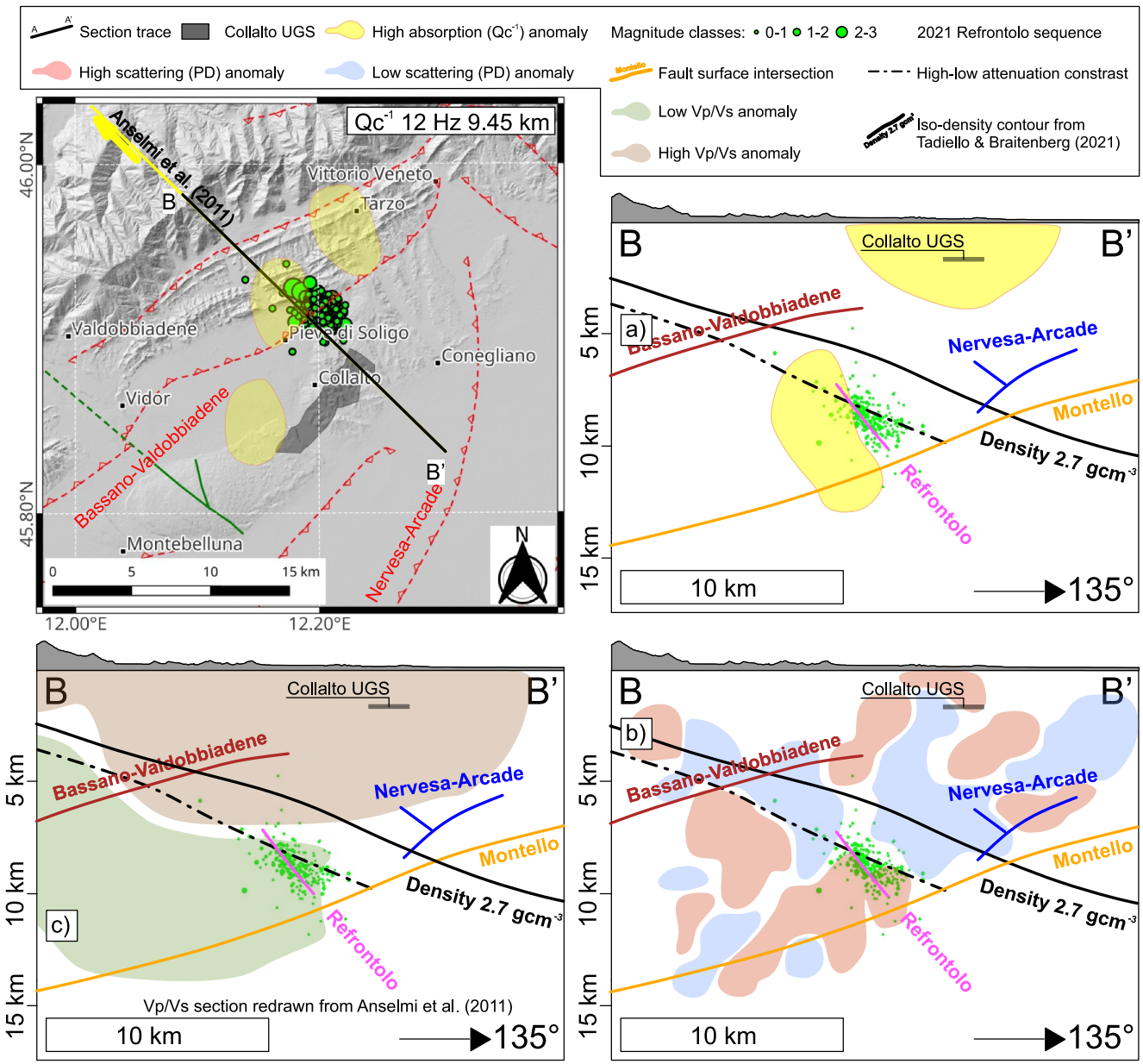

Figure 3. Small-scale absorption and scattering models compared to literature. The anomalies, calculated at a central frequency of 12 Hz, are represented as iso-surfaces, indicating Qc^{-1} values higher than 0.002 (yellow), and PD > 0.05s (red) or < −0.05s (blue). The horizontal slice shows the absorption model at 9.45 km (see Supporting Information S1 for other slices and further methodological details), the BB′ cross-section trace, and the 2021 Refrontolo cluster (Peruzza et al., 2022). Vertical cross-sections are realized in the small-scale model and partially overlap Section 1 in Anselmi et al. (2011) (yellow line in the map); the represented values are: (a) the absorption anomalies, (b) the scattering anomalies, and (c) the *Vp*/*Vs* ratio redrawn from Anselmi et al. (2011). The three cross-sections are overlaid by an identical frame composed of: earthquakes of the Refrontolo cluster projected with a semi-width of 0.5 km and scaled according to the magnitude; fault surface intersections from the 3D structural model illustrated in Figure 1; an iso-density contour from the Tadiello and Braitenberg (2021) model (solid black line, density of 2.7 g/cm^3); the main separation between high and low scattering values (dash-dotted black line); the position of the Collalto Underground Gas Storage (labeled black rectangle).

At finer scales, *PD* becomes more sensitive to lithological contrasts. The high-resolution scattering model reveals a SE-dipping low-*PD* anomaly within the Montello hanging wall (Figure 3b). This feature approximately coincides with a seismic velocity contrast (Anselmi et al., 2011; Figure 3c) and a 3D density model (Tadiello & Braitenberg, 2021; Figure 3, black iso-density contours). The boundary marks the transition between thrust-stacked carbonate units (Bassano–Valdobbiadene and Montello) and the overlying low-density, high *Vp/Vs* sediments of the Venetian Plain. The interface is mostly planar, with local dip variations near faults, consistent with a compressional tectonic setting.

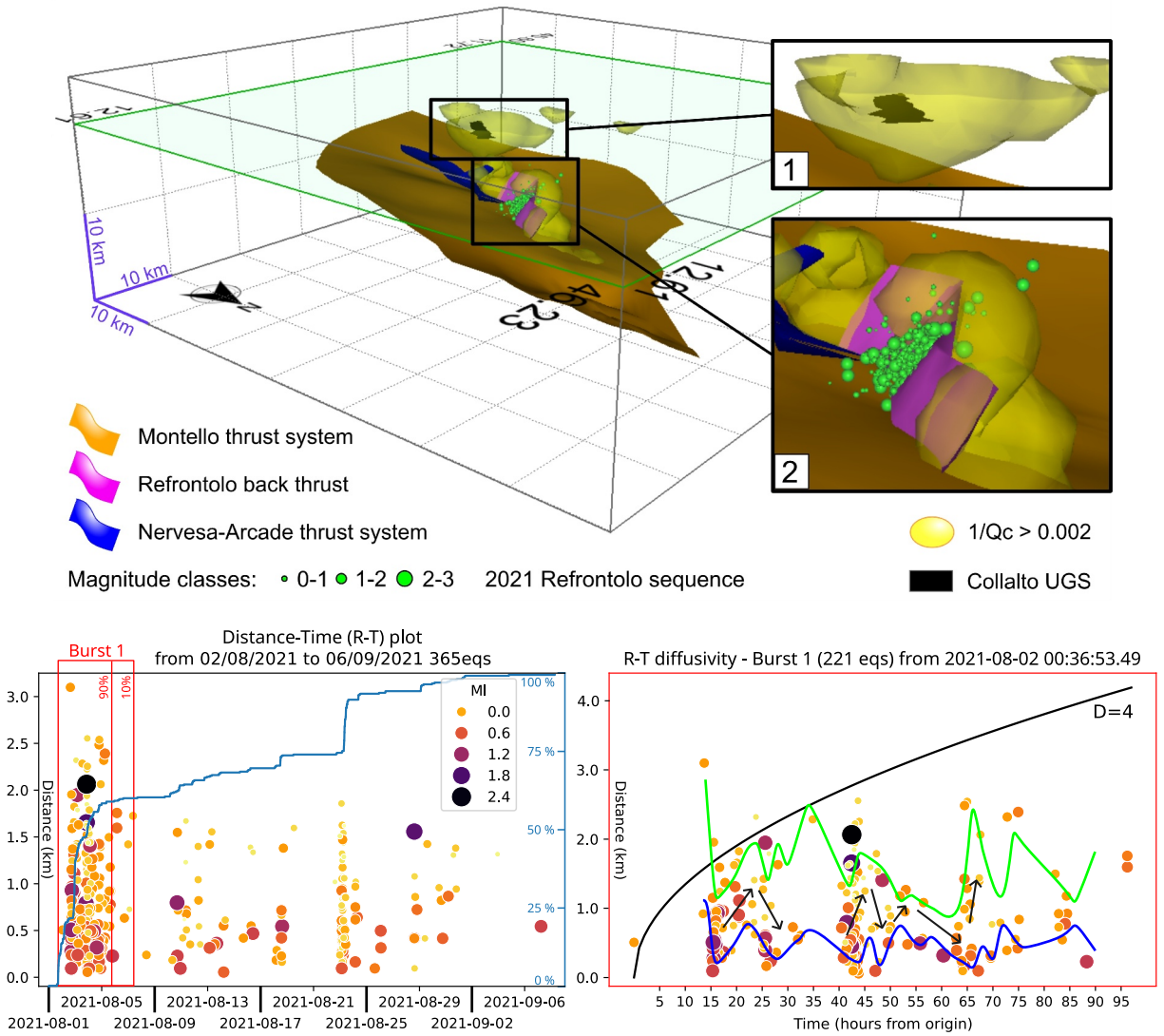

Figure 4. Small-scale absorption model with comparisons to the 2021 Refrontolo cluster. The anomalies are represented as iso-volumes, indicating $Qc^{-1} > 0.002$ (yellow) within the neighboring tectonic structures: the Montello thrust (orange), the Nervesa-Arcade thrust system (blue), and the Refrontolo backthrust (pink). The two zoom images show high absorption anomalies around the Collalto Underground Gas Storage (black polygon in inset 1) and contouring the seismic sequence (green spheres scaled according to the magnitude in inset 2), respectively. The results of the spatiotemporal analysis of seismicity are shown using R-T plots. (left) The Refrontolo sequence and the cumulative number of earthquakes with time (blue line), (right) the first burst event, the diffusivity law (black line), and the seismic front (green) and back front (blue) in a constant 2-hr window (see Text and Figure S14 in Supporting Information S1 for further details).

4.2. Absorption: Fluid Circulation

In contrast to the *PD*, density, and *Vp*/*Vs* models, the seismic absorption model reveals features that do not correlate with mapped structures or lithological boundaries. It shows two distinct anomalies with high-Qc^{-1}: a shallow hemispherical feature in the upper 4 km of the crust and a deeper, more complex anomaly between 6 and 13 km depth (Figure 3a). The shallow anomaly spatially includes the Collalto UGS (Figure 3a; Figure 4, inset 1). We interpret this feature as the result of fluid-induced absorption, confirming the high sensitivity of Qc^{-1} tomography to fluid content and its value for tectonic studies. The Collalto reservoir lies at ∼1.5 km depth and extends ∼8 km NE–SW and ∼1.5 km NW–SE (Romano et al., 2019), whereas the associated high-Qc^{-1} anomaly extend laterally over ∼16 × 8 km and reaches ∼4 km in depth. This size difference likely reflects the limited spatial resolution of the Qc^{-1} model, which is constrained by a node spacing of 1 km. In addition, exploration data (SGI & UNMIG, 2010, Figure S1 in Supporting Information S1) report multiple depleted or unexploited fluid-

bearing layers in the area, suggesting that the observed anomaly may represent a more extensive fluid-rich volume rather than a single reservoir. These interpretations are not mutually exclusive.

The second, deeper high-Qc^{-1} anomaly is located beneath the Refrontolo backthrust (Figure 3a; Figure 4, inset 2), which is top-bounded by a low-scattering region in the hanging wall and by a high-Qc^{-1} zone in the footwall (Figures 3a and 3b). Using the Collalto anomaly as a reference for fluid sensitivity, we interpret this deeper feature as indicating the presence of fluid at depth. Synthetic tests (Figure S13 in Supporting Information S1) confirm the robustness of the anomaly, although geological and geophysical constraints are not yet sufficient to determine its physical nature. This deep anomaly is in a region of frequent microseismic activity, recorded by the Collalto local seismic network. Among these, the 2021 Refrontolo sequence stands out due to its detailed documentation and number of events, providing a seismological signature that supports the presence and dynamic role of fluids inferred from our attenuation model.

The sequence, analyzed by Peruzza et al. (2022), went through at least three burst phases, the first of which included the M_L 2.4 mainshock (Figure 4, R–T plots). During the sequence, a localized increase in the *Vp*/*Vs* ratio (from a background median of 1.78 to 1.85) was observed, a variation commonly interpreted as indicative of fluid involvement in earthquake triggering. The R–T distribution of the first burst phase is consistent with a hydraulic diffusion model (Shapiro et al., 2002), with a best-fit diffusivity of ∼4 m^2/s. Such a value is computed following Amezawa et al. (2021), De Barros et al. (2024), and Díaz-Moreno et al. (2015) (see Figure S14 in Supporting Information S1 for further details).

Using the total seismic moment released during the sequence and the approach of Danré et al. (2022), we estimate the fluid volume involved in triggering at $\sim 1.4 \times 10^4$ m^3. This is comparable to values for naturally triggered seismic swarms and thus supports a fluid-driven interpretation. However, the spatio-temporal evolution of the sequence cannot be fully explained by pure diffusion due to its complexity. In particular, the expansion and retreat of the seismic front and backfront show a non-monotonic behavior, suggesting the involvement of additional mechanisms. We therefore propose a mixed triggering process including pore pressure diffusion, poroelastic stress changes, and static stress transfer as shown by Boyet et al. (2023). Finally, we point out that the size of the volume of the identified anomaly is subject to uncertainty due to limitations in tomographic resolution and interpolation effects and should not be overinterpreted.

Geological processes such as mineral hydrolysis or metamorphic decarbonation can generate CO_2 and other fluids at depth, provided suitable thermal conditions are present (Kissin & Pakhomov, 1975). These fluids in a supercritical state can accumulate in deep crustal reservoirs and migrate upward along tectonic discontinuities, potentially affecting shallower systems (e.g., de Nardis et al., 2024; Smeraglia et al., 2018). In support of this hypothesis, Italiano et al. (2009) documented the persistent release of deeply sourced CO_2 along tectonic structures in the Friuli region. Their interpolated CO_2 map shows elevated concentrations near Pordenone, just east of our study area. By analogy, we suggest that similar processes may occur beneath the Montello thrust system, where compressional tectonics both generate and guide the upward migration of deep fluids.

The reconstructed framework in which fluids likely play a key role in modulating local seismicity along the Montello thrust system is consistent with Anderlini et al. (2020) and Barba et al. (2013), who advanced the hypothesis of creeping behavior based on GPS data and the observations of Romano et al. (2019) on seismicity analyses. We emphasize that such behavior does not exclude larger earthquakes in an active tectonic area, as has been observed in other parts of the world (Lienkaemper et al., 2012).

5. Conclusion

In this work, we present the first multi-scale seismic attenuation tomography of a sector of the eastern SA, focusing on both the regional tectonic setting and the Collalto UGS located inside the Montello hill, to characterize fault structures and detect fluid-related anomalies. The reconstructed attenuation anomalies are associated with both tectonic fractures and the presence of fluids, confirming the overall tectonic setting and the position and isolation of the UGS.

Seismic scattering tomography confirms its effectiveness in mapping fault geometry and stress accumulation zones, being more sensitive to the fractured zones. The coda-based absorption model demonstrates its ability to detect fluid-rich volumes, even in a tectonic context, thereby overcoming the limitations of other geophysical models, such as seismic velocity, *Vp*/*Vs* ratio, or 3D rock density.

Our results suggest that fluids play a central role in modulating seismicity in the Montello system. The detection of a deep high-absorption anomaly beneath the Refrontolo backthrust, together with its spatial correlation to clustered seismicity and anomalous *Vp*/*Vs* variations, supports a fluid-driven triggering process.

These results demonstrate the value of attenuation tomography as a complementary imaging tool in tectonically active areas. By revealing features that cannot be detected with conventional seismic parameters, it provides important insights into fluid-structure interaction and its influence on fault slip and earthquake occurrence.

Conflict of Interest

The authors declare no conflicts of interest relevant to this study.

Data Availability Statement

The workspace used to perform analyses with the open-access MuRAT3D MATLAB© code is available at MuRAT 3.0 (2021). The plots were generated using the Move 3D platform (PetEx Ltd., version, 2022), QGIS software (QGIS.org, 2025), and Inkscape Graphic Editor (Inkscape project, 2020). The data used in this work are available at Romano et al. (2025). Scattering and absorption models produced in this work are available at Talone (2025).

Acknowledgments
We thank Stogit Adriatica S.p.A. (Snam Group) for their contribution to our research. Research activities have been carried out in the frame of the Italian PRIN "Fault segmentation and seismotectonics of active thrust systems: the Northern Apennines and Southern Alps laboratories for new Seismic Hazard Assessments in northern Italy (NASA4SHA)" (PI R. Caputo, UR Responsible L. Peruzza). Open access publishing facilitated by Universita degli Studi Gabriele d'Annunzio Chieti Pescara, as part of the Wiley - CRUI-CARE agreement.

References

Akande, W. G., De Siena, L., & Gan, Q. (2019). Three-dimensional kernel-based coda attenuation imaging of caldera structures controlling the 1982-84 Campi Flegrei unrest. *Journal of Volcanology and Geothermal Research*, *381*, 273–283. https://doi.org/10.1016/j.jvolgeores.2019.06.007

Aki, K., & Chouet, B. (1975). Origin of coda waves: Source, attenuation, and scattering effects. *Journal of Geophysical Research*, *80*(23), 3322–3342. https://doi.org/10.1029/JB080i023p03322

Akinci, A., Munafò, I., & Malagnini, L. (2022). S-Wave attenuation variation and its impact on ground motion amplitudes during 2016–2017 central Italy earthquake sequence. *Frontiers in Earth Science*, *10*, 903955. https://doi.org/10.3389/feart.2022.903955

Akinci, A., Pezzo, E. D., & Malagnini, L. (2020). Intrinsic and scattering seismic wave attenuation in the central Apennines (Italy). *Physics of the Earth and Planetary Interiors*, *303*, 106498. https://doi.org/10.1016/j.pepi.2020.106498

Amezawa, Y., Maeda, T., & Kosuga, M. (2021). Migration diffusivity as a controlling factor in the duration of earthquake swarms. *Earth Planets and Space*, *73*(1), 148. https://doi.org/10.1186/s40623-021-01480-7

Anderlini, L., Serpelloni, E., Tolomei, C., De Martini, P. M., Pezzo, G., Gualandi, A., & Spada, G. (2020). New insights into active tectonics and seismogenic potential of the Italian southern Alps from vertical geodetic velocities. *Solid Earth*, *11*(5), 1681–1698. https://doi.org/10.5194/se-11-1681-2020

Anselmi, M., Govoni, A., De Gori, P., & Chiarabba, C. (2011). Seismicity and velocity structures along the south-Alpine thrust front of the Venetian Alps (NE-Italy). *Tectonophysics*, *513*(1–4), 37–48. https://doi.org/10.1016/j.tecto.2011.09.023

Atterholt, J., Zhan, Z., & Yang, Y. (2022). Fault zone imaging with distributed acoustic sensing: Body-to-surface wave scattering. *Journal of Geophysical Research: Solid Earth*, *127*(11), e2022JB025052. https://doi.org/10.1029/2022JB025052

Barba, S., Finocchio, D., Sikdar, E., & Burrato, P. (2013). Modelling the interseismic deformation of a thrust system: Seismogenic potential of the southern Alps. *Terra Nova*, *25*(3), 221–227. https://doi.org/10.1111/ter.12026

Bigi, G., Castellarin, A., Coli, M., Dal Piaz, G. V., & Vai, G. B. (1990). Structural model of Italy scale 1:500.000, sheet 2. C.N.R., Progetto Finalizzato geodinamica, SELCA Firenze. *Progetto Finalizzato Geodinamica, SELCA Firenze*. Retrieved from https://drive.google.com/file/d/1xGOLP3gxUVEKisBHQc_gBCc13pvYhmQm/view?usp=sharing

Borleanu, F., De Siena, L., Thomas, C., Popa, M., & Radulian, M. (2017). Seismic scattering and absorption mapping from intermediate-depth earthquakes reveals complex tectonic interactions acting in the Vrancea region and surroundings (Romania). *Tectonophysics*, *706–707*, 129–142. https://doi.org/10.1016/j.tecto.2017.04.013

Borleanu, F., Petrescu, L., Seghedi, I., Thomas, C., & De Siena, L. (2023). The seismic attenuation signature of collisional Orogens and sedimentary basins within the Carpathian Orogen. *Global and Planetary Change*, *223*, 104093. https://doi.org/10.1016/j.gloplacha.2023.104093

Boyet, A., De Simone, S., Ge, S., & Vilarrasa, V. (2023). Poroelastic stress relaxation, slip stress transfer and friction weakening controlled post-injection seismicity at the Basel enhanced geothermal system. *Communications Earth & Environment*, *4*(1), 104. https://doi.org/10.1038/s43247-023-00764-y

Burrato, P., Poli, M. E., Vannoli, P., Zanferrari, A., Basili, R., & Galadini, F. (2008). Sources of Mw 5+ earthquakes in northeastern Italy and western Slovenia: An updated view based on geological and seismological evidence. *Tectonophysics*, *453*(1–4), 157–176. https://doi.org/10.1016/j.tecto.2007.07.009

Calvet, M., Sylvander, M., Margerin, L., & Villaseñor, A. (2013). Spatial variations of seismic attenuation and heterogeneity in the Pyrenees: Coda Q and peak delay time analysis. *Tectonophysics*, *608*, 428–439. https://doi.org/10.1016/j.tecto.2013.08.045

Cargioli, A., & Sola, A. (2007). Stoccaggio collalto (TV) ampliamento centrale. (Relazione Tecnico Ambientale No. 06-593-H9).

Castellarin, A., Nicolich, R., Fantoni, R., Cantelli, L., Sella, M., & Selli, L. (2006). Structure of the lithosphere beneath the eastern Alps (southern sector of the TRANSALP transect). *Tectonophysics*, *414*(1–4), 259–282. https://doi.org/10.1016/j.tecto.2005.10.013

Clarke, J., Adam, L., Van Wijk, K., & Sarout, J. (2020). The influence of fluid type on elastic wave velocity and attenuation in volcanic rocks. *Journal of Volcanology and Geothermal Research*, *403*, 107004. https://doi.org/10.1016/j.jvolgeores.2020.107004

Curzi, M., Viola, G., Zuccari, C., Aldega, L., Billi, A., Van Der Lelij, R., et al. (2024). Tectonic evolution of the eastern southern Alps (Italy): A reappraisal from new structural data and geochronological constraints. *Tectonics*, *43*(3), e2023TC008013. https://doi.org/10.1029/2023TC008013

Danré, P., De Barros, L., Cappa, F., & Ampuero, J. (2022). Prevalence of aseismic slip linking fluid injection to natural and anthropogenic seismic swarms. *Journal of Geophysical Research: Solid Earth*, *127*(12), e2022JB025571. https://doi.org/10.1029/2022JB025571

De Barros, L., Danré, P., Garagash, D., Cappa, F., & Lengliné, O. (2024). Systematic observation of a seismic back-front during fluid injection in both natural and anthropogenic earthquake swarms. *Earth and Planetary Science Letters*, *641*, 118849. https://doi.org/10.1016/j.epsl.2024.118849

Del Pezzo, E., De La Torre, A., Bianco, F., Ibanez, J., Gabrielli, S., & De Siena, L. (2018). Numerically calculated 3D space-weighting functions to image crustal volcanic structures using diffuse coda waves. *Geosciences*, *8*(5), 175. https://doi.org/10.3390/geosciences8050175

de Nardis, R., Vuan, A., Carbone, L., Talone, D., Romano, M. A., & Lavecchia, G. (2024). Interplay of tectonic and dynamic processes shaping multilayer extensional system in southern-central Apennines. *Scientific Reports*, *14*(1), 18375. https://doi.org/10.1038/s41598-024-69118-8

De Siena, L., Amoruso, A., Pezzo, E. D., Wakeford, Z., Castellano, M., & Crescentini, L. (2017). Space-weighted seismic attenuation mapping of the aseismic source of Campi Flegrei 1983–1984 unrest. *Geophysical Research Letters*, *44*(4), 1740–1748. https://doi.org/10.1002/2017GL072507

De Siena, L., Calvet, M., Watson, K. J., Jonkers, A. R. T., & Thomas, C. (2016). Seismic scattering and absorption mapping of debris flows, feeding paths, and tectonic units at Mount St. Helens volcano. *Earth and Planetary Science Letters*, *442*, 21–31. https://doi.org/10.1016/j.epsl.2016.02.026

De Siena, L., Thomas, C., & Aster, R. (2014). Multi-scale reasonable attenuation tomography analysis (MuRAT): An imaging algorithm designed for volcanic regions. *Journal of Volcanology and Geothermal Research*, *277*, 22–35. https://doi.org/10.1016/j.jvolgeores.2014.03.009

Díaz-Moreno, A., Ibáñez, J. M., De Angelis, S., García-Yeguas, A., Prudencio, J., Morales, J., et al. (2015). Seismic hydraulic fracture migration originated by successive deep magma pulses: The 2011–2013 seismic series associated to the volcanic activity of El Hierro Island. *Journal of Geophysical Research: Solid Earth*, *120*(11), 7749–7770. https://doi.org/10.1002/2015JB012249

Di Martino, M. D. P., De Siena, L., & Tisato, N. (2022). Pore space topology controls ultrasonic waveforms in dry volcanic rocks. *Geophysical Research Letters*, *49*(18), e2022GL100310. https://doi.org/10.1029/2022GL100310

Fehler, M., Hoshiba, M., Sato, H., & Obara, K. (1992). Separation of scattering and intrinsic attenuation for the Kanto-Tokai region, Japan, using measurements of *S*-wave energy versus hypocentral distance. *Geophysical Journal International*, *108*(3), 787–800. https://doi.org/10.1111/j.1365-246X.1992.tb03470.x

Gabrielli, S., Akinci, A., De Siena, L., Del Pezzo, E., Buttinelli, M., Maesano, F. E., & Maffucci, R. (2023). Scattering attenuation images of the control of thrusts and fluid overpressure on the 2016–2017 central Italy seismic sequence. *Geophysical Research Letters*, *50*(8), e2023GL103132. https://doi.org/10.1029/2023GL103132

Galadini, F., Poli, M. E., & Zanferrari, A. (2005). Seismogenic sources potentially responsible for earthquakes with $M \geq 6$ in the eastern southern Alps (Thiene-Udine sector, NE Italy). *Geophysical Journal International*, *161*(3), 739–762. https://doi.org/10.1111/j.1365-246X.2005.02571.x

Guardo, R., De Siena, L., Prudencio, J., & Ventura, G. (2022). Imaging the absorbing feeding and eruptive pathways of deception island, Antarctica. *Geophysical Research Letters*, *49*(19), e2022GL099540. https://doi.org/10.1029/2022GL099540

Handy, M. R., M. Schmid, S., Bousquet, R., Kissling, E., & Bernoulli, D. (2010). Reconciling plate-tectonic reconstructions of Alpine Tethys with the geological–geophysical record of spreading and subduction in the Alps. *Earth-Science Reviews*, *102*(3–4), 121–158. https://doi.org/10.1016/j.earscirev.2010.06.002

Husen, S., & Hardebeck, J. (2010). Earthquake location accuracy. *Community Online Resource for Statistical Seismicity Analysis*. https://doi.org/10.5078/CORSSA-55815573

Inkscape project. (2020). Inkscape graphic editor [Software]. Retrieved from https://inkscape.org

Italiano, F., Bonfanti, P., Ditta, M., Petrini, R., & Slejko, F. (2009). Helium and carbon isotopes in the dissolved gases of Friuli region (NE Italy): Geochemical evidence of CO_2 production and degassing over a seismically active area. *Chemical Geology*, *266*(1–2), 76–85. https://doi.org/10.1016/j.chemgeo.2009.05.022

ITHACA Working Group. (2019). ITHACA (ITaly HAzard from CApable faulting), A database of active capable faults of the Italian territory [Dataset]. Retrieved from http://sgi2.isprambiente.it/ithacaweb/Mappatura.aspx

King, T., De Siena, L., Benson, P., & Vinciguerra, S. (2023). Mapping faults in the laboratory with seismic scattering 1: The laboratory perspective. *Geophysical Journal International*, *232*(3), 1590–1599. https://doi.org/10.1093/gji/ggac409

King, T., De Siena, L., Zhang, Y., Nakata, N., Benson, P., & Vinciguerra, S. (2023). Mapping faults in the laboratory with seismic scattering 2: The modelling perspective. *Geophysical Journal International*, *234*(2), 1024–1031. https://doi.org/10.1093/gji/ggad100

Kissin, I., & Pakhomov, S. (1975). Some features of the geochemistry Op thermal water in platform areas from experimental data.

Lienkaemper, J. J., McFarland, F. S., Simpson, R. W., Bilham, R. G., Ponce, D. A., Boatwright, J. J., & Caskey, S. J. (2012). Long-term creep rates on the Hayward fault: Evidence for controls on the size and frequency of large earthquakes. *Bulletin of the Seismological Society of America*, *102*(1), 31–41. https://doi.org/10.1785/0120110033

Mavko, G., Mukerji, T., & Dvorkin, J. (2020). *The rock physics handbook* (3rd ed.). Cambridge University Press. https://doi.org/10.1017/9781108333016

Mayor, J., Calvet, M., Margerin, L., Vanderhaeghe, O., & Traversa, P. (2016). Crustal structure of the Alps as seen by attenuation tomography. *Earth and Planetary Science Letters*, *439*, 71–80. https://doi.org/10.1016/j.epsl.2016.01.025

MuRAT 3.0. (2021). LucaDeSiena/MuRAT. Original version from GitHub [Software]. Retrieved from https://github.com/LucaDeSiena/MuRAT

Napolitano, F., De Siena, L., Amoroso, O., Ágústsdóttir, T., Benediktsdóttir, Á., Palo, M., et al. (2025). Scattering and absorption imaging of the Hengill high-temperature geothermal area, southwest Iceland. *Journal of Geophysical Research: Solid Earth*, *130*(5), e2024JB030731. https://doi.org/10.1029/2024JB030731

Napolitano, F., De Siena, L., Gervasi, A., Guerra, I., Scarpa, R., & La Rocca, M. (2020). Scattering and absorption imaging of a highly fractured fluid-filled seismogenetic volume in a region of slow deformation. *Geoscience Frontiers*, *11*(3), 989–998. https://doi.org/10.1016/j.gsf.2019.09.014

Nardoni, C., De Siena, L., Cammarano, F., Magrini, F., & Mattei, E. (2021). Modelling regional-scale attenuation across Italy and the Tyrrhenian Sea. *Physics of the Earth and Planetary Interiors*, *318*, 106764. https://doi.org/10.1016/j.pepi.2021.106764

Nardoni, C., & Persaud, P. (2024). Evidence for faulting and fluid-driven earthquake processes from seismic attenuation variations beneath Los Angeles. *Scientific Reports*, *14*(1), 17595. https://doi.org/10.1038/s41598-024-67872-3

Peruzza, L., Romano, M. A., Guidarelli, M., Moratto, L., Garbin, M., & Priolo, E. (2022). An unusually productive microearthquake sequence brings new insights to the buried active thrust system of Montello (southeastern Alps, northern Italy). *Frontiers in Earth Science*, *10*, 1044296. https://doi.org/10.3389/feart.2022.1044296

PetEx Ltd., version. (2022). MOVE suite software [Software]. Retrieved from https://www.petex.com/products/move-suite/

Picotti, V., Romano, M. A., Ponza, A., Guido, F. L., & Peruzza, L. (2022). The Montello thrust and the active Mountain front of the eastern southern alps (northeast Italy). *Tectonics*, *41*(12), e2022TC007522. https://doi.org/10.1029/2022TC007522

Poli, M. E., Burrato, P., Galadini, F., & Zanferrari, A. (2008). Seismogenic sources responsible for destructive earthquakes in north-eastern Italy. *Bollettino Di Geofisica Teorica e Applicata*, *49*(3–4), 301–313.

Priolo, E., Romanelli, M., Plasencia Linares, M. P., Garbin, M., Peruzza, L., Romano, M. A., et al. (2015). Seismic monitoring of an underground natural gas storage facility: The Collalto seismic network. *Seismological Research Letters*, *86*(1), 109–123. https://doi.org/10.1785/0220140087

Prudencio, J., Ibáñez, J. M., Del Pezzo, E., Martí, J., García-Yeguas, A., & De Siena, L. (2015). 3D attenuation tomography of the volcanic island of Tenerife (Canary Islands). *Surveys in Geophysics*, *36*(5), 693–716. https://doi.org/10.1007/s10712-015-9333-3

QGIS.org. (2025). QGIS geographic information system [Software]. *QGIS Association*. Retrieved from https://qgis.org/

Reiss, M. C., De Siena, L., & Muirhead, J. D. (2022). The interconnected magmatic plumbing system of the natron rift. *Geophysical Research Letters*, *49*(15), e2022GL098922. https://doi.org/10.1029/2022GL098922

Romano, M. A., Peruzza, L., Garbin, M., Priolo, E., & Picotti, V. (2019). Microseismic portrait of the Montello thrust (southeastern alps, Italy) from a dense high-quality seismic network. *Seismological Research Letters*, *90*(4), L10305. https://doi.org/10.1785/0220180387

Romano, M. A., Talone, D., Bernardi, P., Diez Zaldivar, E. R., Franceschinel, F., Garbin, M., et al. (2025). Earthquake dataset used for seismic attenuation tomography in the Montello area (eastern southern Alps, northern Italy) [Dataset]. *Zenodo*. https://doi.org/10.5281/zenodo.15839151

Saito, T., Sato, H., & Ohtake, M. (2002). Envelope broadening of spherically outgoing waves in three-dimensional random media having power law spectra. *Journal of Geophysical Research*, *107*(B5), 2089. https://doi.org/10.1029/2001JB000264

Saraò, A., Sugan, M., Bressan, G., Renner, G., & Restivo, A. (2021). A focal mechanism catalogue of earthquakes that occurred in the south-eastern Alps and surrounding areas from 1928–2019. *Earth System Science Data*, *13*(5), 2245–2258. https://doi.org/10.5194/essd-13-2245-2021

Sato, H. (1989). Broadening of seimogram evelopes in the randomly inhomogeneous lithosphere based in the parabolic approximation: South-estern Honshu, Japan. *Journal of Geophysical Research*, *94*(B12), 17735–17747. https://doi.org/10.1029/jb094ib12p17735

Schurr, B., Asch, G., Rietbrock, A., Trumbull, R., & Haberland, C. (2003). Complex patterns of fluid and melt transport in the central Andean subduction zone revealed by attenuation tomography. *Earth and Planetary Science Letters*, *215*(1–2), 105–119. https://doi.org/10.1016/S0012-821X(03)00441-2

SGI, & UNMIG. (2010). ViDEPI (visibility of petroleum exploration data in Italy). *Italian Journal of Geosciences*, *129*(1), 3.

Shapiro, S. A., Rothert, E., Rath, V., & Rindschwentner, J. (2002). Characterization of fluid transport properties of reservoirs using induced microseismicity. *Geophysics*, *67*(1), 212–220. https://doi.org/10.1190/1.1451597

Sketsiou, P., Napolitano, F., Zenonos, A., & De Siena, L. (2020). New insights into seismic absorption imaging. *Physics of the Earth and Planetary Interiors*, *298*, 106337. https://doi.org/10.1016/j.pepi.2019.106337

Smeraglia, L., Bernasconi, S. M., Berra, F., Billi, A., Boschi, C., Caracausi, A., et al. (2018). Crustal-scale fluid circulation and co-seismic shallow comb-veining along the longest normal fault of the central Apennines, Italy. *Earth and Planetary Science Letters*, *498*, 152–168. https://doi.org/10.1016/j.epsl.2018.06.013

Tadiello, D., & Braitenberg, C. (2021). Gravity modeling of the Alpine lithosphere affected by magmatism based on seismic tomography. *Solid Earth*, *12*(2), 539–561. https://doi.org/10.5194/se-12-539-2021

Takahashi, T., Sato, H., Nishimura, T., & Obara, K. (2009). Tomographic inversion of the peak delay times to reveal random velocity fluctuations in the lithosphere: Method and application to northeastern Japan. *Geophysical Journal International*, *178*(3), 1437–1455. https://doi.org/10.1111/j.1365-246X.2009.04227.x

Talone, D. (2025). Attenuation models in "Underground Gas Storage as benchmark for seismic attenuation tomography in a tectonically complex region (north-eastern Italy)" [Dataset]. https://doi.org/10.5281/zenodo.15791893

Talone, D., De Siena, L., Lavecchia, G., & De Nardis, R. (2023). The attenuation and scattering signature of fluid reservoirs and tectonic interactions in the central-southern Apennines (Italy). *Geophysical Research Letters*, *50*(22), e2023GL106074. https://doi.org/10.1029/2023GL106074

Tisato, N., Quintal, B., Chapman, S., Podladchikov, Y., & Burg, J. (2015). Bubbles attenuate elastic waves at seismic frequencies: First experimental evidence. *Geophysical Research Letters*, *42*(10), 3880–3887. https://doi.org/10.1002/2015GL063538

Villani, F., Antonioli, A., Pastori, M., Baccheschi, P., & Ciaccio, M. G. (2024). Stress patterns and crustal anisotropy in the eastern Alps: Insights from seismological and geological observations. *Tectonics*, *43*(3), e2023TC008033. https://doi.org/10.1029/2023TC008033

Visini, F., de Nardis, R., Barbano, M. S., & Lavecchia, G. (2009). Testing the seismogenic sources of the January 11th 1693 Sicilian earthquake (Io X/XI): Insights from macroseismic field simulations. *Italian Journal of Geosciences*, *128*(1), 147–156.

Visini, F., de Nardis, R., & Lavecchia, G. (2010). Rates of active compressional deformation in central Italy and Sicily: Evaluation of the seismic budget. *International Journal of Earth Sciences*, *99*(S1), 243–264. https://doi.org/10.1007/s00531-009-0473-x

Yemane, T., Kendall, J. M., Gabrielli, S., & De Siena, L. (2025). Mapping geothermal fluids using seismic absorption and scattering: A case study from Aluto volcano. *Geophysical Research Letters*, *52*(19), e2025GL115364. https://doi.org/10.1029/2025gl115364

Zhu, Z., Bezada, M. J., Byrnes, J. S., & Ford, H. A. (2021). Evidence for stress localization caused by lithospheric heterogeneity from seismic attenuation. *Geochemistry, Geophysics, Geosystems*, *22*(11), e2021GC009987. https://doi.org/10.1029/2021GC009987

References From the Supporting Information

Aster, R. C., Thurber, C. H., & Borchers, B. (2005). *Parameter estimation and inverse problems, international geophysics series*. Elsevier Academic Press.

Michele, M., Latorre, D., & Emolo, A. (2019). An empirical formula to classify the quality of earthquake locations. *Bulletin of the Seismological Society of America*, *109*(6), 2755–2761. https://doi.org/10.1785/0120190144